

Journal homepage: <https://modernpathology.org/>

Research Article

The Involvement of PI3K–Akt Signaling in the Clinical and Pathological Findings of Idiopathic Multicentric Castleman Disease–Thrombocytopenia, Anasarca, Fever, Reticulin Fibrosis, and Organomegaly and Not Otherwise Specified Subtypes

Tomoka Haratake^a, Midori Filiz Nishimura^a, Asami Nishikori^a, Michael V. Gonzalez^b, Daisuke Ennishi^{c,d}, You Cheng Lai^e, Sayaka Ochi^a, Manaka Tsunoda^a, David C. Fajgenbaum^{b,f}, Frits van Rhee^g, Shuji Momose^h, Yasuharu Sato^{a,*}

^a Department of Molecular Hematopathology, Okayama University Graduate School of Health Sciences, Okayama, Japan; ^b Center for Cytokine Storm Treatment and Laboratory, Department of Medicine, Perelman School of Medicine, University of Pennsylvania, Philadelphia, Pennsylvania; ^c Center for Comprehensive Genomic Medicine, Okayama University Hospital, Okayama, Japan; ^d Department of Hematology and Oncology, Okayama University Hospital, Okayama, Japan; ^e Department of Medical Biotechnology and Laboratory Science, Chang Gung University, Taoyuan, Taiwan; ^f Castleman Disease Collaborative Network, Philadelphia, Pennsylvania; ^g Myeloma Center, University of Arkansas for Medical Sciences, Little Rock, Arkansas; ^h Department of Pathology, Saitama Medical Center, Saitama Medical University, Saitama, Japan

ARTICLE INFO

Article history:

Received 30 January 2025

Revised 11 April 2025

Accepted 12 April 2025

Available online 22 April 2025

Keywords:

idiopathic multicentric Castleman disease

integrin subunit alpha 5

PI3K–Akt signaling pathway

platelet-derived growth factor

receptor beta

vascular endothelial growth factor A

vascularity

ABSTRACT

Idiopathic multicentric Castleman disease is a rare lymphoproliferative disorder that is clinically classified into idiopathic plasmacytic lymphadenopathy (IPL); thrombocytopenia, anasarca, fever, reticulin fibrosis, and organomegaly (TAFRO); and not otherwise specified (NOS). Although each subtype shows varying degrees of hypervascularity, no statistical data on the degree of vascularization have been reported. Additionally, the mechanisms underlying vascularization in each clinical subtype are poorly understood. Here, we aimed to clarify these mechanisms by evaluating the histopathological characteristics of each clinical subtype across 37 patients and performing a whole-transcriptome analysis focusing on angiogenesis-related gene expression. Histologically, TAFRO and NOS exhibited a significantly higher degree of vascularization than IPL (IPL vs TAFRO, $P < .001$; IPL vs NOS, $P = .002$). In addition, the germinal centers (GCs) were significantly more atrophic in TAFRO than in IPL. In TAFRO and NOS, "whirlpool vessels" in GCs were seen in most cases (TAFRO, 9/9, 100%; NOS, 6/8, 75%) but not in IPL (IPL vs TAFRO, $P < .001$; IPL vs NOS, $P = .007$). Likewise, immunostaining for Ets-related gene revealed higher levels in endothelial cells of GCs in TAFRO than in IPL ($P = .014$), and TAFRO and NOS were associated with a significantly higher number of endothelial cells in interfollicular areas compared with that in IPL (TAFRO vs IPL, $P < .001$; NOS vs IPL, $P = .002$). Gene expression analysis revealed that the PI3K–Akt signaling pathway was significantly enriched in the TAFRO and NOS (TAFRO/NOS) groups. This pathway, which may be activated by vascular endothelial growth factor A and some integrins, is known to affect angiogenesis by increasing vascular permeability, which may explain the clinical manifestations of anasarca and/or fluid retention in TAFRO/NOS. These results suggest that the PI3K–Akt pathway plays an important role in the pathogenesis of TAFRO/NOS.

© 2025 THE AUTHORS. Published by Elsevier Inc. on behalf of the United States & Canadian Academy of Pathology. This is an open access article under the CC BY license (<http://creativecommons.org/licenses/by/4.0/>).

* Corresponding author.

E-mail address: satou-y@okayama-u.ac.jp (Y. Sato).



Introduction

Kaposi sarcoma-associated herpesvirus/human herpesvirus type 8-negative idiopathic multicentric Castleman disease (iMCD) is a rare lymphoproliferative disorder characterized by systemic inflammation of unknown etiology.^{1,2} It is clinically classified into 3 subtypes: idiopathic plasmacytic lymphadenopathy (IPL); thrombocytopenia, anasarca, fever, reticulin fibrosis/renal dysfunction, and organomegaly (TAFRO); and not otherwise specified (NOS).³⁻⁶ Each clinical subtype is known to exhibit varying degrees of vascularization⁷⁻¹⁰ but the pathological mechanisms are not well understood, and available data are limited. The PI3K–Akt–mTOR pathway has been previously implicated, but the exact role that it plays within specific iMCD subtypes is unknown.¹¹ Likewise, the role of angiogenesis in disease etiology and progression is not understood. Here, we hypothesized that differences in dysregulated signaling pathways associated with angiogenesis between the subtypes may contribute to clinical characteristics such as pleural effusions and ascites seen in TAFRO and often NOS cases. Therefore, we aimed to objectively examine the degree of vascularization and differences in angiogenesis-related gene expression in each subtype performed via immunohistochemical staining and whole-transcriptome analysis of lymph node tissue.

Materials and Methods

Patient Selection

All patients included in this study showed histologic findings consistent with iMCD and were serologically or immunohistochemically negative for herpesvirus/human herpesvirus type 8.¹² iMCD subtyping was performed using clinical criteria.^{4,7,13} We defined iMCD-IPL as a case meeting 3 criteria: (1) prominent polyclonal hypergammaglobulinemia (gamma globulin > 4.0 g/dL or serum immunoglobulin G level > 3500 mg/dL), (2) multiple lymphadenopathy, and (3) the absence of a definite autoimmune disease.^{4,13} TAFRO was defined according to the criteria provided in a previous report⁷: (T) thrombocytopenia (pretreatment nadir platelet level $\leq 100 \times 10^3/\mu\text{L}$), (A) anasarca, (F) fever or hyperinflammatory status (fever $\geq 37.5^\circ\text{C}$ of unknown etiology or C-reactive protein $>2.0 \text{ mg/dL}$), (R) renal insufficiency (pretreatment estimated glomerular filtration rate $\leq 60 \text{ mL/minutes}/1.73 \text{ m}^2$, creatinine $>1 \text{ mg/dL}$ [female]/ $>1.3 \text{ mg/dL}$ [male], or renal failure necessitating hemodialysis) or TAFRO-consistent bone marrow features (reticulin fibrosis or megakaryocytic hyperplasia, without evidence of an alternative diagnosis), and (O) organomegaly. NOS was defined as cases that met the iMCD diagnostic criteria but not the IPL or TAFRO criteria.^{4,7,12,13}

The Institutional Review Board of Okayama University approved this study (protocol number: 2007-033), which was performed in accordance with the tenets of the Declaration of Helsinki.

Histopathological Evaluation

Lymph node specimens from 9 IPL, 9 TAFRO, and 8 NOS cases were fixed in 10% neutral-buffered formalin solution and embedded in paraffin. Paraffin-embedded tissue blocks were sliced into 3- μm sections and stained with hematoxylin and eosin. The histopathological features of vascularity and plasmacytosis

were graded on a score of 0 to 3 based on a previous report¹² (*Supplementary Fig. S1A*). Germinal center (GC) status was scored based on the frequency of hyperplastic GCs observed (*Supplementary Fig. S1A*). A score of 0 was defined as no GC formation or atrophic GCs only, and the score was increased with increasing hyperplastic GC frequency. For all cases, these features were reviewed by 2 authors (Y.S. and T.H.). Discussions were held until an agreement was reached regarding discrepancies in their assessments. In addition, we evaluated the presence or absence of “whirlpool vessels” in the GCs, defined as endothelial cells aligning in a whirlpool-like arrangement, showing directional flow (*Supplementary Fig. S1B*).¹⁴ All assessments were performed on whole specimens. All specimens evaluated in this study were obtained from biopsies taken for diagnosis. However, 2 patients with IPL had already received tocilizumab, 1 NOS patient prednisolone (PSL), 2 patients with TAFRO received PSL, and 1 TAFRO case received PSL and tocilizumab. Histopathological findings were compared statistically among the IPL, TAFRO, and NOS groups.

Immunohistochemical Staining

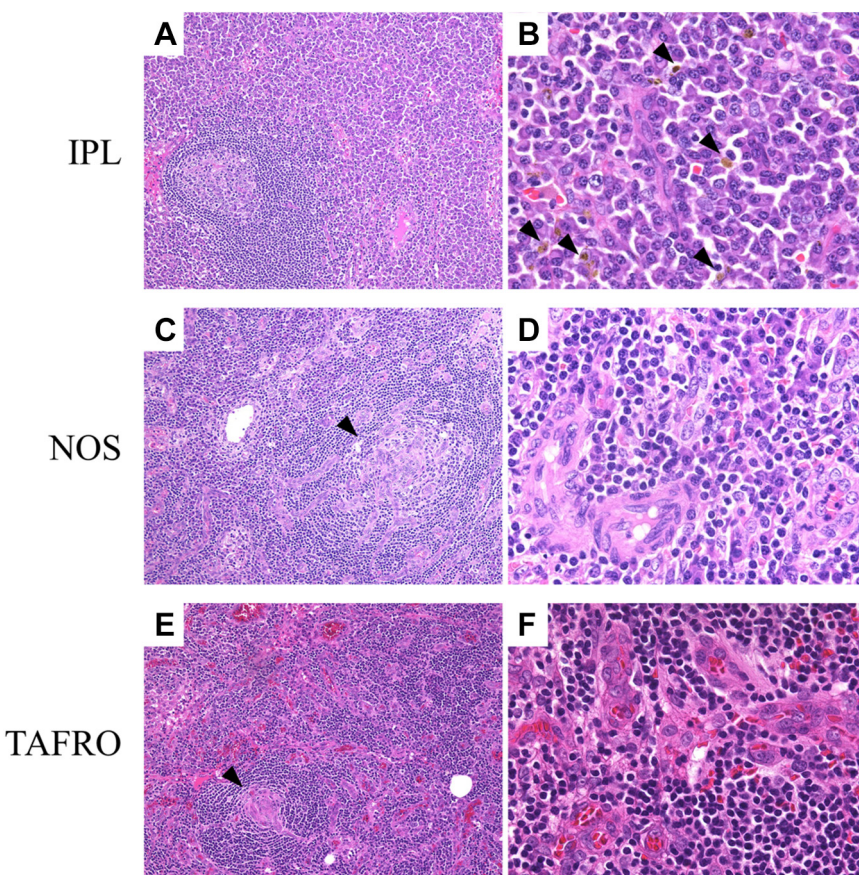
Immunohistochemical staining was performed on 8 IPL, 9 TAFRO, and 7 NOS samples using an automated BOND-III instrument (Leica Biosystems) with anti-Ets-related gene (ERG) primary antibody (OTI4H7, MA5-26245, 1:200 dilution; Thermo Fisher Scientific). The number of ERG-positive cells was counted in the GCs and interfollicular areas in 5 high-power fields (OLYMPUS BX50, field number: 26.5) using ImageJ (version 1.54g; National Institutes of Health, Bethesda).¹⁵ Immunohistochemical staining results were compared statistically among the IPL, TAFRO, and NOS groups.

Gene Expression Analysis

Total RNA was extracted from 12, 2, and 4 IPL, TAFRO, and NOS frozen specimens, respectively, using an RNeasy Tissue Mini Kit (Qiagen) according to the manufacturer's instructions. RNA was quantified using an Agilent 2100 Bioanalyzer (Agilent Technologies). Following processing using the poly A method, the remaining RNAs were fragmented using a fragmentation buffer and reverse transcribed into complementary DNA with random primers. RNA sequencing (RNA-seq) was performed using a NovaSeq 6000 system (Illumina).¹⁶ Differentially expressed genes (DEGs) between the TAFRO/NOS and IPL groups were assessed using edgeR package (version 4.2.1)¹⁷ and defined based on a false discovery rate $\leq .05$ and absolute \log_2 fold change ≥ 1.5 . Kyoto Encyclopedia of Genes and Genomes (KEGG) pathway enrichment analysis was performed for upregulated DEGs in TAFRO/NOS versus IPL using the clusterProfiler package (version 4.12.1) to identify gene expression associated with angiogenesis.^{18,19} In this analysis, we used the same data from a previous report indicating that IPL is a uniform subtype in terms of gene expression,²⁰ whereas TAFRO and NOS exhibit clinicopathological and gene expression overlap.^{5,20} Therefore, for DEG identification and KEGG pathway enrichment analysis, comparisons were made between the IPL group and the TAFRO/NOS group.

Statistical Analysis

To analyze histopathology scoring and transcriptome analysis data, Mann–Whitney *U* and Steel tests were used for comparisons

**Figure 1.**

Histopathological findings for each subtype. (A, B) IPL case with vascularity score 0, GC status score 3, and plasmacytosis score 3. (A) Hyperplastic GCs with minimal vascularization were observed ($\times 100$). (B) Sheet-like proliferation of mature plasma cells and deposition of hemosiderin (arrowhead) were observed ($\times 400$). (C, D) NOS case scored as vascularity score 3, GC status score 1, and plasmacytosis score 1. (C) Whirlpool vessels were observed (arrowhead) ($\times 100$). (D) Marked vascularization with enlarged nuclei in the endothelium and proliferation of mature plasma cells were seen in interfollicular areas ($\times 400$). (E, F) TAFRO case scored as vascularity score 3, GC status score 0, and plasmacytosis score 0. (E) Whirlpool vessels in atrophic GCs (arrowhead) ($\times 100$). (F) Marked vascularization with enlarged nuclei in the endothelium and absence of mature plasma cell proliferation in interfollicular areas ($\times 400$). GC, germinal center; IPL, idiopathic plasmacytic lymphadenopathy; NOS, not otherwise specified; TAFRO, thrombocytopenia, anasarca, fever, reticulin fibrosis, and organomegaly.

between 2 and 3 groups, respectively. Fisher exact test was used to evaluate pathological findings. All P values were calculated from 2-sided tests, and statistical significance was set using a threshold of $P < .05$. The P values were adjusted as needed using the Benjamini–Hochberg procedure in edgeR. All statistical analyses were performed using R (version 4.4.1; <https://cran.r-project.org>).

Results

Histopathological Evaluation

Upon histopathological evaluation, lymph node tissue from patients with TAFRO and NOS exhibited significantly higher hypervascularity scores compared with IPL tissues (IPL vs TAFRO, $P < .001$; IPL vs NOS, $P = .002$), with no statistical difference between TAFRO and NOS. In addition, whirlpool vessels were frequently observed in atrophic GCs in TAFRO (9/9, 100%) and NOS (6/8, 75%) but never in IPL (IPL vs TAFRO, $P < .001$; IPL vs NOS, $P = .007$). TAFRO and NOS samples received lower plasmacytosis scores than IPL samples (IPL vs TAFRO, $P < .001$; IPL vs NOS, $P = .020$), again with no difference between TAFRO and NOS. IPL GCs showed significantly higher GC status scores than those in

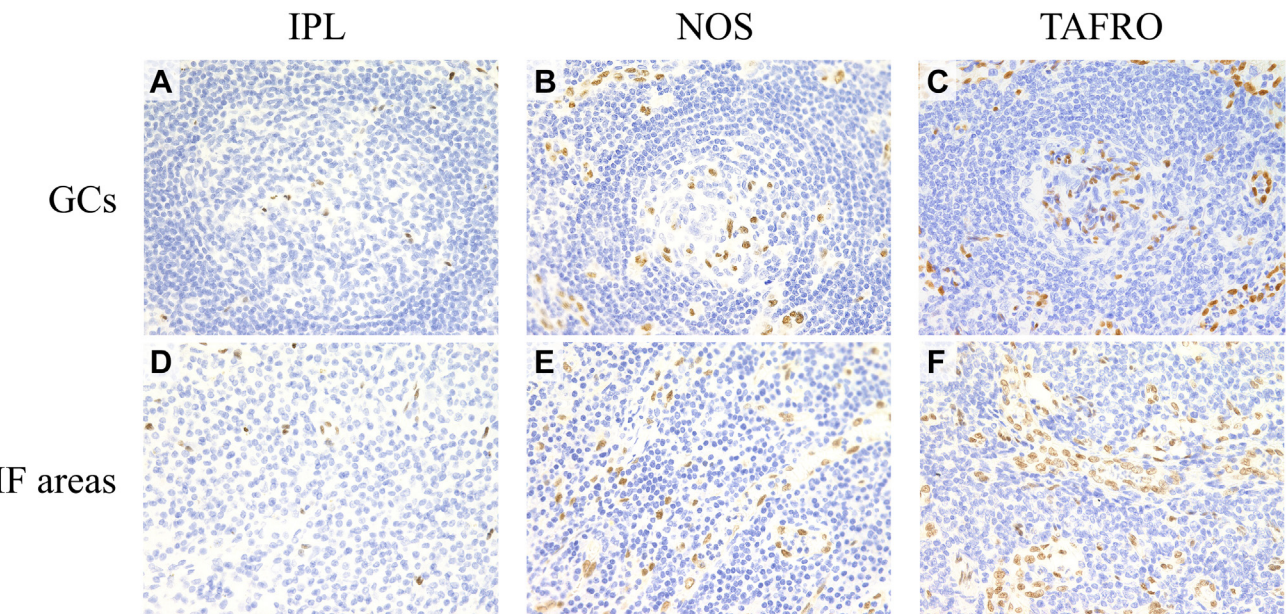
TAFRO ($P = .011$), but NOS samples showed no significant differences from either IPL or TAFRO samples (Supplementary Table S1). Typical histologic findings for each subtype are shown in Figure 1.

Immunohistochemical Staining

Figures 2 and 3 present the results of ERG immunohistochemical staining in each iMCD subtype. The number of ERG-positive cells in the GCs of TAFRO samples was significantly higher than that in IPL samples ($P = .014$); however, no difference was observed among other subtypes (Figs 2A–C and 3). In interfollicular areas, the number of ERG-positive cells in TAFRO and NOS samples was significantly higher than that in IPL samples (TAFRO, $P < .001$; NOS, $P = .002$), with no difference between TAFRO and NOS (Figs. 2D–F and 3).

Gene Expression Analysis

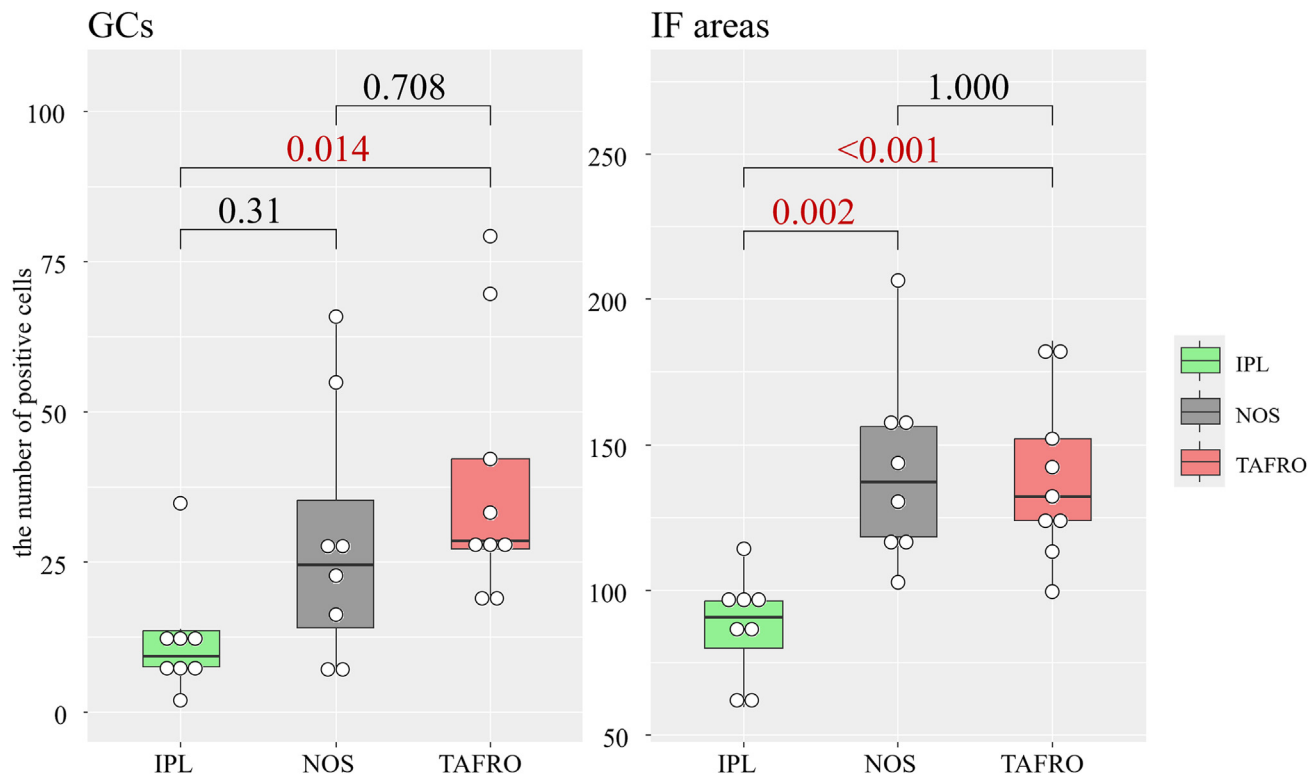
To identify potential signaling pathways and gene sets that may be associated with the increased vascularity, we performed

**Figure 2.**

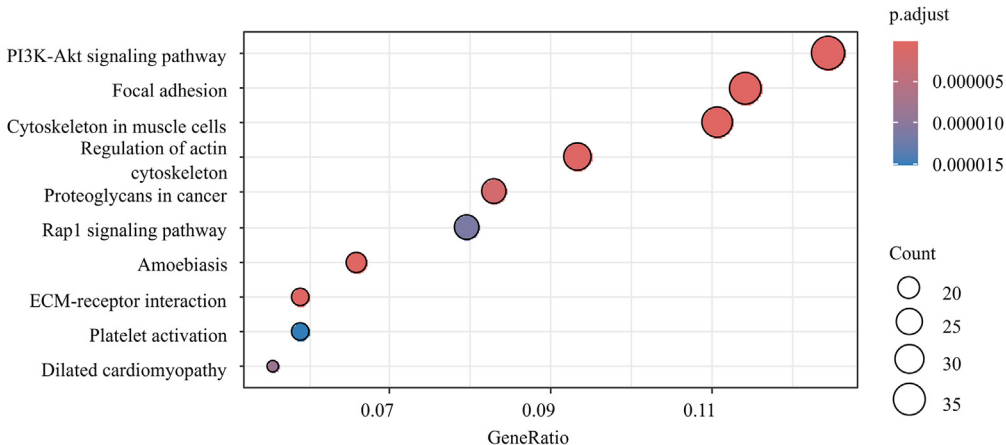
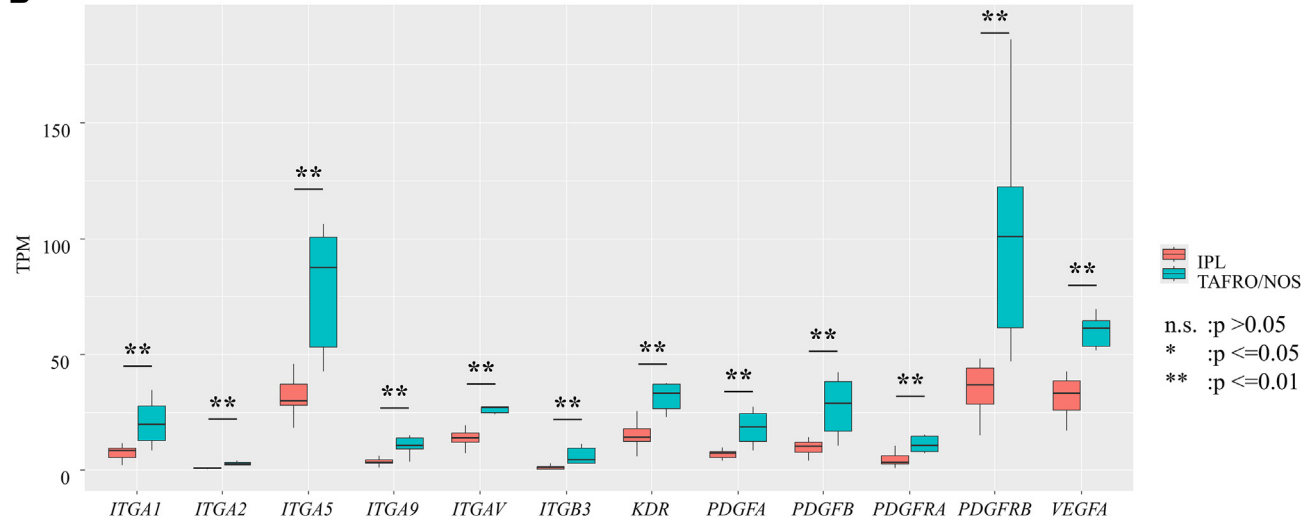
Ets-related gene (ERG) immunohistochemical staining for vascularity in each subtype. ERG immunohistochemical staining in (A-C) germinal centers (GCs) and (D-F) interfollicular (IF) areas from IPL (A, D), TAFRO (B, E), and NOS (C, F) samples (400 \times). IPL, idiopathic plasmacytic lymphadenopathy; NOS, not otherwise specified; TAFRO, thrombocytopenia, anasarca, fever, reticulin fibrosis, and organomegaly.

pathway analysis using RNA-seq data from lymph node tissue. We used data that we previously published from 12 patients with IPL, 2 patients with TAFRO, and 4 patients with NOS, which showed

common gene expression between TAFRO and NOS, and as such, these cases were combined.²⁰ Differential expression analysis revealed 596 upregulated and 113 downregulated genes in TAFRO/

**Figure 3.**

Number of Ets-related gene (ERG)-positive cells in each subtype. Box-and-whisker and dot plots of ERG-positive cell counts in germinal centers (GCs) and interfollicular (IF) areas, with comparisons between patient groups. The number of ERG-positive cells is the average of the absolute counts in 5 high-power fields. P values in red indicate significant differences; those in black are nonsignificant. Significance was calculated using the Mann-Whitney U test. IPL, idiopathic plasmacytic lymphadenopathy; NOS, not otherwise specified; TAFRO, thrombocytopenia, anasarca, fever, reticulin fibrosis, and organomegaly

A**B****Figure 4.**

Transcriptome analysis. (A) Top 10 Kyoto Encyclopedia of Genes and Genomes pathway enrichment in TAFRO/NOS tissues. The color of the circle indicates the adjusted P value. The size of the circle indicates the number of differentially expressed genes (DEGs) contained in each of its pathways. (B) Expression of DEGs upstream of the PI3K–Akt signaling pathway. The blue box plot shows the gene expression values of the IPL group, whereas the red box plot shows those of the TAFRO/NOS group. Significance was calculated using the Mann–Whitney U test. IPL, idiopathic plasmacytic lymphadenopathy; NOS, not otherwise specified; n.s., not significant; TAFRO, thrombocytopenia, anasarca, fever, reticular fibrosis, and organomegaly; ECM, extracellular matrix; TPM, transcripts per million. * $P \leq 0.05$, ** $P \leq 0.01$.

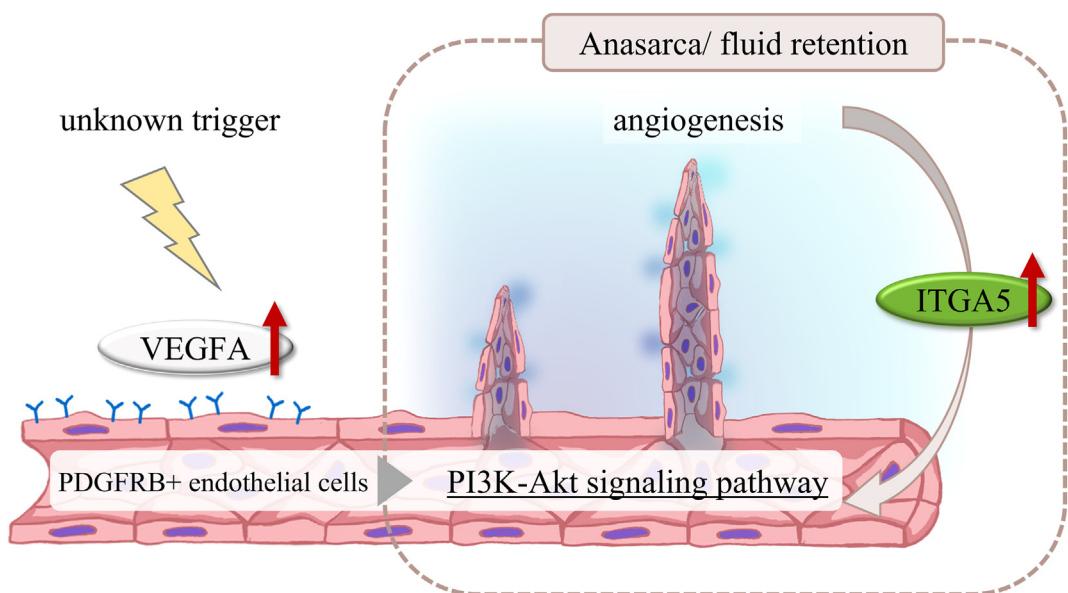
NOS compared with IPL (Supplementary Fig. S2 and Supplementary Table S2), including several with important roles in vascular development, such as *vascular endothelial growth factor A* (*VEGFA*) and *platelet-derived growth factor receptor beta* (*PDGFRB*).

We performed KEGG enrichment analysis of the DEGs between TAFRO/NOS and IPL and found that the PI3K–Akt signaling pathway was the most enriched in TAFRO/NOS (Fig. 4A and Supplementary Fig. S3), the group with prominent vascularization. Upstream DEGs related to this pathway included *platelet-derived growth factor A* (*PDGFA*), *PDGFB*, *PDGFRA*, *PDGFRB*, *VEGFA*, *kinase insert domain receptor*, and several *integrins*. Among those genes, *VEGFA*, *PDGFRB*, and *integrin subunit alpha* (*ITGA5*) showed particularly high expression (Fig. 4B). Although genes related to the RAS–RAF1–ERK pathway were not upregulated, those of the eNOS–PKG–p38–ERK pathway were upregulated in TAFRO/NOS samples relative to their expression in IPL samples (Supplementary Fig. S4). Although genes related to the eNOS–PKG–p38–ERK pathway had log fold-change values below the threshold and were not included as DEGs, significant differences in their expression were observed between the IPL and TAFRO/NOS groups.

Discussion

In this study, we analyzed the degree of vascularization and the expression of angiogenesis-related genes in lymph node tissues from each iMCD clinical subtype. Histopathological findings, including vascularity, plasmacytosis, and GC status, in TAFRO/NOS were statistically different from those in IPL. Additionally, we examined the presence of whirlpool vessels for the first time across the 3 subtypes and found that this characteristic served as a distinguishing feature between IPL and TAFRO/NOS. This pattern of angiogenesis in GCs may be influenced by the DEGs identified in this study and/or the unique environment of the GCs, but evidence is limited.

Gene expression analysis revealed that genes related to the PI3K–Akt signaling pathway were significantly enriched in the TAFRO/NOS group relative to the IPL group. Furthermore, *VEGFA*, *PDGFRB*, and *ITGA5* showed particularly high expression. As *VEGFA* and *ITGA5* are known to activate the PI3K–Akt signaling pathway,^{21–24} our findings suggest that these factors induce PI3K–Akt signaling in TAFRO/NOS. Indeed, previous reports have

**Figure 5.**

Proposed mechanism of angiogenesis in thrombocytopenia, anasarca, fever, reticulin fibrosis, and organomegaly and not otherwise specified. In response to inflammation, increased levels of vascular endothelial growth factor A (VEGFA) and platelet-derived growth factor receptor beta (PDGFRB) in vascular endothelial cells may activate the PI3K–Akt signaling pathway, leading to angiogenesis and increased vascular permeability in thrombocytopenia, anasarca, fever, reticulin fibrosis, and organomegaly and not otherwise specified subtypes. In addition, some integrins derived from neovascularized blood vessels may further activate the PI3K–Akt pathway and cause prominent anasarca and/or fluid retention. ITGA5, integrin subunit alpha.

documented high serum VEGFA levels in patients with iMCD (overall or TAFRO/NOS groups).^{25,26} VEGFA is known to enhance vascular permeability and promote angiogenesis,^{24,27,28} corresponding to the clinical features of TAFRO/NOS. Downstream of VEGFA, the RAS–RAF1–ERK pathway strongly promotes angiogenesis, and the PI3K–Akt–eNOS–PKG–p38–ERK pathway modulates the extent of angiogenesis by suppressing the RAS–RAF1–ERK pathway and enhances vascular permeability.^{23,24,29–32} We hypothesize that strongly enriched PI3K–Akt–eNOS–PKG–p38–ERK signaling suppresses RAS–RAF1–ERK signaling in TAFRO/NOS. Furthermore, PDGFRB overexpression has been reported to strongly activate the PI3K–Akt signaling pathway.^{33,34} In normal tissues, PDGFRB is predominantly expressed in vascular pericytes, with minimal expression in vascular endothelial cells, except in tumors or inflammatory conditions.^{34,35} Furthermore, high VEGFA expression indirectly inhibits the recruitment of vascular pericytes.³⁶ Thus, the recruitment of vascular pericytes, which support vascular endothelial cells and inhibit vascular permeability, to developing vessels may be suppressed.³⁷ Therefore, the high expression of PDGFRB and VEGFA observed in the TAFRO/NOS group in this study may indicate inflammation, PI3K–Akt activation, and vascular pericyte recruitment inhibition, providing insights into disease pathogenesis. PDGFRB is known to bind not only PDGF but also VEGFA.^{38,39} Additionally, the VEGFA–PDGFRB binding affinity is stronger than that of PDGF–PDGFRB.³⁹ Therefore, the enrichment of the PI3K–Akt signaling pathway may be particularly strongly influenced by the strong VEGFA–PDGFRB interaction. ITGA5, which is expressed in platelets and endothelial cells,⁴⁰ showed high expression in TAFRO/NOS in this study. ITGA5 plays a vital role in angiogenesis and activates the PI3K–Akt signaling pathway.^{21,22,41} Therefore, the high ITGA5 expression observed here may reflect an increase in endothelial cells and further activation of the PI3K–Akt signaling pathway. This is potentially related to the hypervascularization in affected lesions and the

clinical severity of symptoms such as anasarca and/or fluid retention, which are characteristic of TAFRO and often NOS cases.^{7,14,20,24} PI3K–Akt signaling pathway activation is also known to induce platelet apoptosis.⁴² In addition, high PDGFRB expression in bone marrow stromal cells is known to be associated with severe myelofibrosis.^{43–45} Therefore, the activation of PI3K and the high expression of PDGFRB in the bone marrow of patients with TAFRO may lead to thrombocytopenia and reticulin fibrosis.

Our results suggest that targeting the PI3K–Akt signaling pathway, potentially upstream of mTOR, may be a valid therapeutic target for TAFRO/NOS. Indeed, studies have reported some success in treating TAFRO by targeting mechanistic target of rapamycin kinase inhibitors located downstream of the PI3K–Akt signaling pathway.^{11,26,46} Inhibiting PI3K and other molecules located upstream of the mechanistic target of rapamycin kinase may also exert therapeutic effects.

We also focused on interleukin 6 (IL-6), a cytokine upstream of the PI3K–Akt pathway that plays an essential role in the pathogenesis of iMCD, particularly IPL.^{4,14} However, there was no difference in IL-6 gene expression between the IPL and TAFRO/NOS groups ($P = .892$). In addition, previous reports have shown no difference in serum IL-6 levels between these groups.^{14,47} This suggests that the PI3K–Akt pathway is affected by cytokines other than IL-6. Because TAFRO causes cytokine storms,²⁰ which subsequently increase IL-6 levels, we believe that gene expression and serum IL-6 levels may be increased in TAFRO as well as IPL.

This study had several limitations. First, identifying specific cells that activate the PI3K–Akt signaling pathway was not possible because we performed bulk RNA-seq. However, both histopathology and immunohistochemical staining suggested a difference in vascular endothelial cell features when comparing TAFRO/NOS and IPL. Therefore, we speculate that vascular endothelial cells are responsible at least in part for the PI3K–Akt signaling pathway activation. Second, the power of DEG detection

in gene transcripts was limited because of the small number of TAFRO/NOS cases investigated.

In conclusion, we demonstrated increased vascularity in TAFRO/NOS iMCD subtypes and identified a possible mechanism. We propose that elevated *VEGFA* and *PDGFRB* expression in vascular endothelial cells in response to inflammation may activate the PI3K–Akt signaling pathway and induce angiogenesis in TAFRO/NOS with increased permeability. Furthermore, some integrins derived from neovascularized blood vessels may further activate the PI3K–Akt signaling pathway and cause prominent anasarca and/or fluid retention (Fig. 5). To validate these hypotheses, future studies using spatial transcriptomics and single-cell analysis may be necessary.

Author Contributions

T.H., A.N., M.F.N., and Y.S. contributed to conceptualization; T.H. contributed to methodology, formal analysis, and writing—original draft; T.H., A.N., M.F.N., D.E., Y.C.L., S.O., T.M., and S.M. contributed to investigation; T.H. and A.N. data curation; A.N., M.F.N., M.V.G., D.C.F., F.v.R., and Y.S. writing—review and editing; A.N., M.F.N., and Y.S. supervised. All authors have read and agreed to the published version of the manuscript.

Data Availability

The data that support the findings of this study are available from the corresponding author, Y.S., upon reasonable request.

Funding

This work was partially supported by JSPS KAKENHI Grant Numbers JP23K14476 and JP24KK0172, JP25K02476, MHLW Program Grant Number JPMH23FC1025; and AMED under Grant Number JP24ek0109589.

Declaration of Competing Interest

The authors declare that they have no known competing financial interests or personal relationships that could have appeared to influence the work reported in this paper.

Ethics Approval and Consent to Participate

The Institutional Review Board of Okayama University approved this study (protocol number 2007-033), which was performed in accordance with the tenets of the Declaration of Helsinki.

Supplementary Material

The online version contains supplementary material available at <https://doi.org/10.1016/j.modpat.2025.100782>.

References

1. Simpson D. Epidemiology of Castleman disease. *Hematol Oncol Clin North Am*. 2018;32(1):1–10. <https://doi.org/10.1016/j.hoc.2017.09.001>
2. Nishimura MF, Nishimura Y, Nishikori A, Yoshino T, Sato Y. Historical and pathological overview of Castleman disease. *J Clin Exp Hematop*. 2022;62(2):60–72. <https://doi.org/10.3960/jslrt.21036>
3. Wang HW, Pittaluga S, Jaffe ES. Multicentric Castleman disease: where are we now? *Semin Diagn Pathol*. 2016;33(5):294–306. <https://doi.org/10.1053/j.semdp.2016.05.006>
4. Takeuchi K. Idiopathic plasmacytic lymphadenopathy: a conceptual history along with a translation of the original Japanese article published in 1980. *J Clin Exp Hematop*. 2022;62(2):79–84. <https://doi.org/10.3960/jslrt.22011>
5. Nishimura Y, Nishikori A, Sawada H, et al. Idiopathic multicentric Castleman disease with positive antiphospholipid antibody: atypical and undiagnosed autoimmune disease? *J Clin Exp Hematop*. 2022;62(2):99–105. <https://doi.org/10.3960/jslrt.21038>
6. Nishimura Y, Nishimura MF, Sato Y. International definition of iMCD-TAFRO: future perspectives. *J Clin Exp Hematop*. 2022;62(2):73–78. <https://doi.org/10.3960/jslrt.21037>
7. Nishimura Y, Fajgenbaum DC, Pierson SK, et al. Validated international definition of the thrombocytopenia, anasarca, fever, reticulin fibrosis, renal insufficiency, and organomegaly clinical subtype (TAFRO) of idiopathic multicentric Castleman disease. *Am J Hematol*. 2021;96(10):1241–1252. <https://doi.org/10.1002/ajh.26292>
8. Wu D, Lim MS, Jaffe ES. Pathology of Castleman disease. *Hematol Oncol Clin North Am*. 2018;32(1):37–52. <https://doi.org/10.1016/j.hoc.2017.09.004>
9. Iwaki N, Fajgenbaum DC, Nabel CS, et al. Clinicopathologic analysis of TAFRO syndrome demonstrates a distinct subtype of HHV-8-negative multicentric Castleman disease. *Am J Hematol*. 2016;91(2):220–226. <https://doi.org/10.1002/ajh.24242>
10. Gao YH, Liu YT, Zhang MY, et al. Idiopathic multicentric Castleman disease (iMCD)-idiopathic plasmacytic lymphadenopathy: a distinct subtype of iMCD-not otherwise specified with different clinical features and better survival. *Br J Haematol*. 2024;204(5):1830–1837. <https://doi.org/10.1111/bjh.19334>
11. Fajgenbaum DC, Langan RA, Japp AS, et al. Identifying and targeting pathogenic PI3K/AKT/mTOR signaling in IL-6-blockade-refractory idiopathic multicentric Castleman disease. *J Clin Invest*. 2019;129(10):4451–4463. <https://doi.org/10.1172/JCI126091>
12. Fajgenbaum DC, Uldrick TS, Bagg A, et al. International, evidence-based consensus diagnostic criteria for HHV-8-negative/idiopathic multicentric Castleman disease. *Blood*. 2017;129(12):1646–1657. <https://doi.org/10.1182/blood-2016-10-746933>
13. Mori S, Mohri N. Clinicopathological analysis of systemic nodal plasmacytosis with severe polyclonal hyperimmunoglobulinemia. *Proc Jpn Soc Pathol*. 1978;67:252–253.
14. Nishikori A, Nishimura MF, Nishimura Y, et al. Idiopathic plasmacytic lymphadenopathy forms an independent subtype of idiopathic multicentric Castleman disease. *Int J Mol Sci*. 2022;23(18):10301. <https://doi.org/10.3390/ijms231810301>
15. Schneider CA, Rasband WS, Eliceiri KW. NIH Image to ImageJ: 25 years of image analysis. *Nat Methods*. 2012;9(7):671–675. <https://doi.org/10.1038/nmeth.2089>
16. Modi A, Vai S, Caramelli D, Lari M. The illumina sequencing protocol and the NovaSeq 6000 system. *Methods Mol Biol*. 2021;2242:15–42. https://doi.org/10.1007/978-1-0716-1099-2_2
17. Robinson MD, McCarthy DJ, Smyth GK. edgeR: a bioconductor package for differential expression analysis of digital gene expression data. *Bioinformatics*. 2010;26(1):139–140. <https://doi.org/10.1093/bioinformatics/btp616>
18. Yu G, Wang LG, Han Y, He QY. clusterProfiler: an R package for comparing biological themes among gene clusters. *Omics*. 2012;16(5):284–287. <https://doi.org/10.1089/omi.2011.0118>
19. Kanehisa M, Furumichi M, Sato Y, Ishiguro-Watanabe M, Tanabe M. KEGG: integrating viruses and cellular organisms. *Nucleic Acids Res*. 2021;49(D1):D545–D551. <https://doi.org/10.1093/nar/gkaa970>
20. Nishikori A, Nishimura MF, Tomida S, et al. Transcriptome analysis of the cytokine storm-related genes among the subtypes of idiopathic multicentric Castleman disease. *J Clin Exp Hematop*. 2024;64:297–306. <https://doi.org/10.3960/jslrt.24061>
21. Guidetti GF, Canobbio I, Torti M. PI3K/Akt in platelet integrin signaling and implications in thrombosis. *Adv Biol Regul*. 2015;59:36–52. <https://doi.org/10.1016/j.jbiol.2015.06.001>
22. Estevez B, Du X. New concepts and mechanisms of platelet activation signaling. *Physiology (Bethesda)*. 2017;32(2):162–177. <https://doi.org/10.1152/physiol.00020.2016>
23. Li Z, Zhang G, Feil R, Han J, Du X. Sequential activation of p38 and ERK pathways by cGMP-dependent protein kinase leading to activation of the platelet integrin alphaIIb beta3. *Blood*. 2006;107(3):965–972. <https://doi.org/10.1182/blood-2005-03-1308>
24. Karar J, Maity A. PI3K/AKT/mTOR pathway in angiogenesis. *Front Mol Neurosci*. 2011;4:51. <https://doi.org/10.3389/fnmol.2011.00051>
25. Horna P, King RL, Jevremovic D, Fajgenbaum DC, Dispenzieri A. The lymph node transcriptome of unicentric and idiopathic multicentric Castleman disease. *Haematologica*. 2023;108(1):207–218. <https://doi.org/10.3324/haematol.2021.280370>
26. Sumiyoshi R, Koga T, Kawakami A. Candidate biomarkers for idiopathic multicentric Castleman disease. *J Clin Exp Hematop*. 2022;62(2):85–90. <https://doi.org/10.3960/jslrt.22010>

27. Peach CJ, Mignone VW, Arruda MA, et al. Molecular pharmacology of VEGF-A isoforms: binding and signalling at VEGFR2. *Int J Mol Sci.* 2018;19(4):1264. <https://doi.org/10.3390/ijms19041264>

28. Zachary I. VEGF signalling: integration and multi-tasking in endothelial cell biology. *Biochem Soc Trans.* 2003;31(Pt 6):1171–1177. <https://doi.org/10.1042/bst0311171>

29. Sarg NH, Zaher DM, Abu Jayab NN, Mostafa SH, Ismail HH, Omar HA. The interplay of p38 MAPK signaling and mitochondrial metabolism, a dynamic target in cancer and pathological contexts. *Biochem Pharmacol.* 2024;225, 116307. <https://doi.org/10.1016/j.bcp.2024.116307>

30. Buscà R, Pouysségur J, Lenormand P. ERK1 and ERK2 map kinases: specific roles or functional redundancy? *Front Cell Dev Biol.* 2016;4:53. <https://doi.org/10.3389/fcell.2016.00053>

31. Melincovici CS, Boşca AB, Şuşman S, et al. Vascular endothelial growth factor (VEGF) – key factor in normal and pathological angiogenesis. *Rom J Morphol Embryol.* 2018;59(2):455–467.

32. Chen G, Hitomi M, Han J, Stacey DW. The p38 pathway provides negative feedback for Ras proliferative signaling. *J Biol Chem.* 2000;275(50): 38973–38980. <https://doi.org/10.1074/jbc.M002856200>

33. Wang H, Yin Y, Li W, et al. Over-expression of PDGFR- β promotes PDGF-induced proliferation, migration, and angiogenesis of EPCs through PI3K/Akt signaling pathway. *PLoS One.* 2012;7(2):e30503. <https://doi.org/10.1371/journal.pone.0030503>

34. Kazlauskas A. PDGFs and their receptors. *Gene.* 2017;614:1–7. <https://doi.org/10.1016/j.gene.2017.03.003>

35. Battegay EJ, Thommen R, Humar R, Masahiro A, Syuichi O. Platelet-Derived Growth Factor and Angiogenesis. *Trends Glycosci Glycotechnol.* 1996;8(42): 231–251. <https://doi.org/10.4052/tigg.8.231>

36. Darden J, Payne LB, Zhao H, Chappell JC. Excess vascular endothelial growth factor-A disrupts pericyte recruitment during blood vessel formation. *Angiogenesis.* 2019;22(1):167–183. <https://doi.org/10.1007/s10456-018-9648-z>

37. Goddard LM, Iruela-Arispe ML. Cellular and molecular regulation of vascular permeability. *Thromb Haemost.* 2013;109(3):407–415. <https://doi.org/10.1160/TH12-09-0678>

38. Ball SG, Shuttleworth CA, Kiely CM. Vascular endothelial growth factor can signal through platelet-derived growth factor receptors. *J Cell Biol.* 2007;177(3):489–500. <https://doi.org/10.1083/jcb.200608093>

39. Mamer SB, Chen S, Weddell JC, et al. Discovery of high-affinity PDGF-VEGFR interactions: redefining RTK dynamics. *Sci Rep.* 2017;7(1):16439. <https://doi.org/10.1038/s41598-017-16610-z>

40. Jun Y. Integrins. *J Thromb Hemost.* 2015;26(1):3–9. <https://doi.org/10.2491/jjth.26.3>

41. Smolenski A. Novel roles of cAMP/cGMP-dependent signaling in platelets. *J Thromb Haemost.* 2012;10(2):167–176. <https://doi.org/10.1111/j.1538-7836.2011.04576.x>

42. Yang HX, Li YJ, He YL, Jin KK, Lyu LN, Ding HG. Hydrogen sulfide promotes platelet autophagy via PDGFR- α /PI3K/Akt signaling in cirrhotic thrombocytopenia. *J Clin Transl Hepatol.* 2024;12(7):625–633. <https://doi.org/10.14218/JCTH.2024.00101>

43. Bedekovics J, Kiss A, Beke L, Károlyi K, Méhes G. Platelet derived growth factor receptor-beta (PDGFR β) expression is limited to activated stromal cells in the bone marrow and shows a strong correlation with the grade of myelofibrosis. *Virchows Arch.* 2013;463(1):57–65. <https://doi.org/10.1007/s00428-013-1434-0>

44. Kramer F, Dernedde J, Mezheyevskii A, Tauber R, Micke P, Kappert K. Platelet-derived growth factor receptor β activation and regulation in murine myelofibrosis. *Haematologica.* 2020;105(8):2083–2094. <https://doi.org/10.3324/haematol.2019.226332>

45. Bedekovics J, Szeghalmy S, Beke L, Fazekas A, Méhes G. Image analysis of platelet derived growth factor receptor-beta (PDGFR β) expression to determine the grade and dynamics of myelofibrosis in bone marrow biopsy samples. *Cytometry B Clin Cytom.* 2014. <https://doi.org/10.1002/cytob.21167>

46. Arenas DJ, Floess K, Kobrin D, et al. Increased mTOR activation in idiopathic multicentric Castleman disease. *Blood.* 2020;135(19):1673–1684. <https://doi.org/10.1182/blood.2019002792>

47. Iwaki N, Gion Y, Kondo E, et al. Elevated serum interferon γ -induced protein 10 kDa is associated with TAFRO syndrome. *Sci Rep.* 2017;7:42316. <https://doi.org/10.1038/srep42316>